

Mitochondrial Dysfunction and Tissue Alterations of Ultraviolet-Irradiated Skin in Five Different Mice Strains

Adrián Friedrich, Mariela Paz, Eliana Cela, Juliana Leoni and Daniel Gonzalez Maglio*

Instituto de Estudios de la Inmunidad Humoral (IDEHU – CONICET)/Cátedra de Inmunología, Facultad de Farmacia y Bioquímica, Universidad de Buenos Aires, Junín 956 4th floor (1113), Buenos Aires, Argentina

Abstract: Ultraviolet radiation (UVR) effects on skin have been extensively studied. Several mice strains have been used worldwide in photobiology and photoimmunology studies. Recently, we have developed a method based on flow cytometry in order to analyze mitochondrial dysfunction and superoxide (O_2^-) production *ex vivo* in keratinocytes isolated from irradiated-mice. This method can be helpful to evaluate mitochondrial alterations in different mice models.

In this work, we aimed to compare epidermal response to UVR in five mice strains, both pigmented and albino as well as hairy and hairless strains (SKH:1, Balb/c, C57/BL, DBA/2N and Swiss). Keratinocytes mitochondrial alterations, epidermal hyperplasia and inflammatory mediators' production (epidermis and serum) were determined 72 hours after a 400 mJ/cm² UV dose.

All strains showed epidermal hyperplasia and loss of mitochondrial polarization after irradiation, differing in the magnitude of the response. However, there were significant differences in the basal mitochondrial polarization between strains, showing that the metabolic state of keratinocytes may vary between them. Moreover, mitochondrial O_2^- production was induced in SKH:1 and Balb/c after irradiation, whereas in DBA/2N, Swiss and C57/BL it was at the same level or even lower than in the non-irradiated control. Finally, an increase in inflammatory mediators was only detected in the serum of C57/BL and Swiss mice and in the epidermis of DBA/2N and C57/BL.

Results show that each mice strain has particular characteristics related to cellular metabolism, which may lead to particular responses to UVR exposure. Therefore, the use of a particular mice strain in photobiology models should be carefully considered.

Keywords: Mitochondrial function, Inflammation, UV irradiation, epidermis, keratinocytes.

INTRODUCTION

Ultraviolet radiation (UVr) included in sunlight is one of the most important environmental carcinogens. It includes UVA (320-400 nm), UVB (280-320 nm) and UVC (below 280 nm) radiations, the latter completely blocked by stratospheric ozone. UVr has plenty of effects on exposed cells, from molecular modifications (such as urocanic acid isomerization) to organelles' and cellular alterations (mitochondrial depolarization and apoptotic cell death) [1-4]. The most exposed organ to UVr is the skin, and particularly the epithelia of the skin: the epidermis, composed by keratinocytes (up to 95% of the total cells), melanocytes, Langerhans cells and T lymphocytes. Acute exposure of keratinocytes to UVr leads to inflammation, epidermal thinning with an ulterior hyperplasia, mitochondrial depolarization, reactive oxygen and nitrogen species production and apoptotic cell death (due to DNA damage) through p53 activation, Bax/Bcl-2 balance alteration and mitochondrial release of cytochrome c [5-8]. Chronic exposure may lead to failures in the elimination of altered cells and continuous production

of mediators that promote keratinocytes' proliferation, such as Prostaglandin E₂. Both events can ultimately generate keratinocytes-derived tumors, such as Squamous Cell Carcinoma and Basal Cell Carcinoma [9, 10].

As it was mentioned, mitochondrial alterations and inflammatory skin response are important UVr-induced effects. In our laboratory we have studied mitochondrial damage in epidermis-isolated mitochondria (*in vivo* model), in keratinocytes' culture (*in vitro* model) and, recently, in freshly epidermis-isolated cells (*ex vivo* model) [5, 6, 11]. *In vitro* and *ex vivo* models were developed using fluorescent probes to assess mitochondrial polarization (DiOC₆) and mitochondrial superoxide anion (O_2^-) production (MitoSOX or dihydroethidium) by flow cytometry. The *ex vivo* model is particularly useful since mice are exposed to UVr (allowing *in vivo* tissular and cellular interactions) and after the adequate time, epidermal cells are isolated and immediately analyzed. Outer mitochondrial membrane polarization reflects the metabolic capacity of cell populations. Regarding the inflammatory response, there are key cytokines produced by keratinocytes after UVr. Among them, TNF- α and IL-6 are characteristic pro-inflammatory cytokines that are increased not only in epidermis, but also in the sera of exposed animals [12, 13].

*Address correspondence to this author at the Instituto de Estudios de la Inmunidad Humoral (IDEHU – CONICET)/Cátedra de Inmunología, Facultad de Farmacia y Bioquímica, Universidad de Buenos Aires, Junín 956 4th floor (1113), Buenos Aires, Argentina; Tel: (5411) 4964-8259; Fax: (5411) 4964-0024; E-mail: danielgm@ffyb.uba.ar

In humans, UVr effects on skin greatly depend on the skin type of the exposed individual. According to the pigmentation level of the skin, human beings are more or less susceptible to sunburn and photodamage [14]. However, even the darker phototypes suffer skin malignancies related to UVr exposure [15]. In spite of this fact, the pigmentation of mice strains is not usually considered in animal models. Photodamage has been evaluated both in pigmented (i.e. C57 or DBA) and albino (i.e. Balb/c or SKH:1) mice strain models, without an exhaustive comparison between mice strains responses. Recently, Sharma *et al.* published a comparative study on the skin response to UVr in C57, Balb/c and SKH:1 mice [16]. They demonstrated different responses between mice strain in the transcription of TNF- α and dermal collagen content, but no differences in epidermal hyperplasia and epidermal and dermal glycosaminoglycans and hialuronic acid contents. Previously, Noonan and Hoffman described three phenotypes with different susceptibilities to UVr-induced immunosuppression: highly susceptible mice (C57/B strain among them), lowly susceptible mice (Balb/c among others) and intermediately susceptible (DBA among them) [17].

The aim of this study was to compare epidermal alterations (epidermal hyperplasia, mitochondrial polarization and mitochondrial O₂⁻ production) and inflammatory response (TNF- α and IL-6 in epidermis and serum) of five mice strains (SKH:1, C57/BL, Swiss, Balb/c and DBA/2N) 72 hours after the exposure to 400 mJ/cm² of UVr. We found that keratinocytes' metabolic basal state (mitochondrial polarization in control mice) differs between mice strains, being SKH:1 and Balb/c the most and DBA/2N the less active ones. Moreover, SKH:1 and Balb/c were also the strains with the greatest increase in mitochondrial O₂⁻ production. Finally, and agreeing with the results from Sharma *et al.*, C57/BL was the strain with the strongest inflammatory response after UVr exposure. These results reinforce the idea of reviewing the mice model to be used for photodamage evaluation.

MATERIALS AND METHODS

Animal Models and UV Irradiation

SKH:1 hairless mice were purchased from Charles River Laboratories and reproduced in our facilities. C57/BL, Balb/c and DBA/2N mice were purchased from Comisión Nacional de Energía Atómica – Centro Atómico Ezeiza. Swiss mice were purchased from Universidad de Buenos Aires - Facultad de Farmacia y

Bioquímica. All animals were housed in quarters with 12/12 h light/dark cycle and maintained with water and food *ad libitum*. Three days prior to the irradiation procedure, hair from the back of all mice was completely removed using an electrical clipper and commercial depilatory cream. SKH:1 hairless mice were also treated with depilatory cream in order to produce comparable results.

Female 8 weeks old mice were irradiated on their back with UV light using an 8W UVM-28 Mid-Range Wave (302 nm) lamp from Ultraviolet Products (UVP, Upland, CA, USA), which emits most of its energy within the UVB range (emission spectrum 280-370 nm) peaking at 302 nm and including a 20-30% amount of UVA. The lamp was calibrated with a UVX radiometer (UVP), and its power was determined as 1.1 mWatt/cm². Mice were exposed 6 min and 4 sec to generate a dose of 400 mJ/cm² of UV. Seventy two hours after irradiation mice were bled by submaxillary puncture [18] and sacrificed using a CO₂ gas chamber. Two 8 mm diameter skin samples were taken from the back of each mouse, one for flow cytometry analysis and the other one for histological analysis. Total dorsal skin was separated in order to obtain tissue extracts. For all mice strains used a non-irradiated control group was included, treated in the same fashion that the irradiated one. For all the experiments the number of animals per group was five.

Animals were used in compliance with the research animal use guidelines and with the EC Directive 86/609/EEC [19].

Histological Analysis

Skin samples for histological analysis were fixed with 4% neutral formalin and embedded in white paraffin. Five μ m paraffin sections were prepared and stained with hematoxylin and eosin. Three independent measurements of epidermal thickness were performed in 2 different slides per mice. The observation and photography were performed using an Olympus BX-51 microscope (Olympus, Center Valley, PA, USA) with a Q-color 3 Olympus digital camera. Epidermal thickness was measured with Image Pro 5.1.0.2 for Windows (Media Cybernetics, Bethesda, MD, USA).

Mitochondrial Alterations Analysis

Skin samples obtained from each mouse were incubated with Dispase 25 mg/ml (Invitrogen, Carlsbad, CA, USA) in phosphate saline buffer (PBS) for 2 h at

37°C. Next, the epidermis was separated from the dermis and mechanically disrupted with a tissue homogenizer (Thomas Scientific, New Jersey, NJ, USA) in 1 ml of PBS supplemented with 10% of fetal bovine serum to obtain an epidermal cell suspension which was filtrated through a 50 µm nylon mesh. Cells were stained with DiOC₆ 30 nm (Sigma-Aldrich, St. Louis, MO, USA) and MitoSOX Red 5 µm (Molecular Probes, Invitrogen). Data were acquired on a PAS III PARTEC flow cytometer (Partec, Görlitz, Germany) and analyzed using Cyflogic software (CyFlo Ltd., Turku, Finland).

Epidermal Homogenate Preparation and Cytokines Quantification

Epidermal homogenates were prepared by immersing whole dorsal skin in a 60°C water bath during 30 sec, then the epidermis was scraped from the dermis using a blade. Each epidermis was homogenized individually in 1 ml of PBS, with 0.5 mg/ml EDTA and 0.174 µg/ml PMSF (Sigma Chemical Co.) using a tissue homogenizer (Bio-Gen PRO200, Pro Scientific), then centrifuged at 4°C for 15 min at 10,000 xg. Afterwards, supernatant was isolated and total protein concentration was measured using the BCA Protein Assay Reagent kit (BCA, Pierce Biotechnology, Rockford, IL, USA). Finally, the epidermal extracts were stored at -70°C until cytokine quantification. Mouse TNF-α and IL-6 in epidermal extracts and serum samples were quantified using non-competitive ELISA assays (BD Biosciences, San José, CA, USA). Values were expressed as pg/ml for serum samples and as pg/mg of protein in the case of epidermal extracts.

Statistical Analysis

All values are presented as the mean ± SD. For control vs. irradiated group comparison, the statistical significance was evaluated using Student t-test (if data fulfilled normality and homoscedasticity) or Mann-

Whitney test (if data did not fulfill normality and/or homoscedasticity). For multiple groups comparison, statistical significance was evaluated by a parametric one way analysis of variance (ANOVA) with a Student-Newman-Keuls post-test (if data fulfilled normality and homoscedasticity) or a nonparametric ANOVA with a Dunn post-test (if data did not fulfill normality and/or homoscedasticity). Graphical and statistical analyses were performed with GraphPad Prism 5.0 (GraphPad software, La Jolla, CA, USA), and GraphPad Instat 2.0 (GraphPad software) respectively.

RESULTS

Results from epidermal cellular characteristics (epidermal thickness, DiOC₆⁺ cells, MitoSOX⁺ cells and double positive cells) studied in control animals of the five mice strains are summarized in Table 1. For each characteristic, individual and extended illustrations are described hereafter.

Epidermal Thickness

Figure 1 shows one representative photomicrograph of an H&E stained skin sample of one control and one irradiated mouse of each mice strain. Quantification of epidermal thickness, performed in five samples per group, is shown in a bar graph beside the microphotographs. All mice strains responded with a remarkable keratinocyte proliferation 72 hs after irradiation. Epidermal hyperplasia was statistically greater in all irradiated groups, compared to the corresponding control groups. Basal epidermal thickness (control groups) ranged between 14.0 µm (Balb/c) and 23.3 µm (DBA/2N), without statistically significant differences among them (Table 1).

Mitochondrial Polarization

Figure 2 shows representative histograms of total epidermal cells' green fluorescence (DiOC₆ probe) of one control and one irradiated mouse of each mice

Table 1: Summary of epidermal characteristics in control mice of the five strains studied. Data were analyzed using a parametric (*) or a non-parametric (#) ANOVA, according to the fulfillment of normality and homoscedasticity. Different letters indicate statistically significant differences between groups; while same letters indicate no significant differences (p<0.05; n=5)

	SKH:1	C57/BL	Swiss	Balb/c	DBA/2N
Epidermal Thickness (µm) *	22.9±6.5 ^a	14.9±5.2 ^a	15.3±4.9 ^a	14.0±1.9 ^a	23.3±5.5 ^a
DiOC ₆ ⁺ cells (%) *	66.4±9.4 ^c	48.3±2.8 ^b	50.5±8.6 ^b	78.4±6.6 ^d	33.8±9.4 ^a
MitoSOX ⁺ cells (%) *	19.5±8.0 ^a	35.7±15.5 ^b	32.6±6.8 ^b	11.7±3.7 ^a	51.1±5.7 ^c
MitoSOX ⁺ DiOC ₆ ⁺ cells (%) #	3.3±3.1 ^a	9.2±3.8 ^a	6.2±2.3 ^a	2.7±1.4 ^a	5.7±0.8 ^a

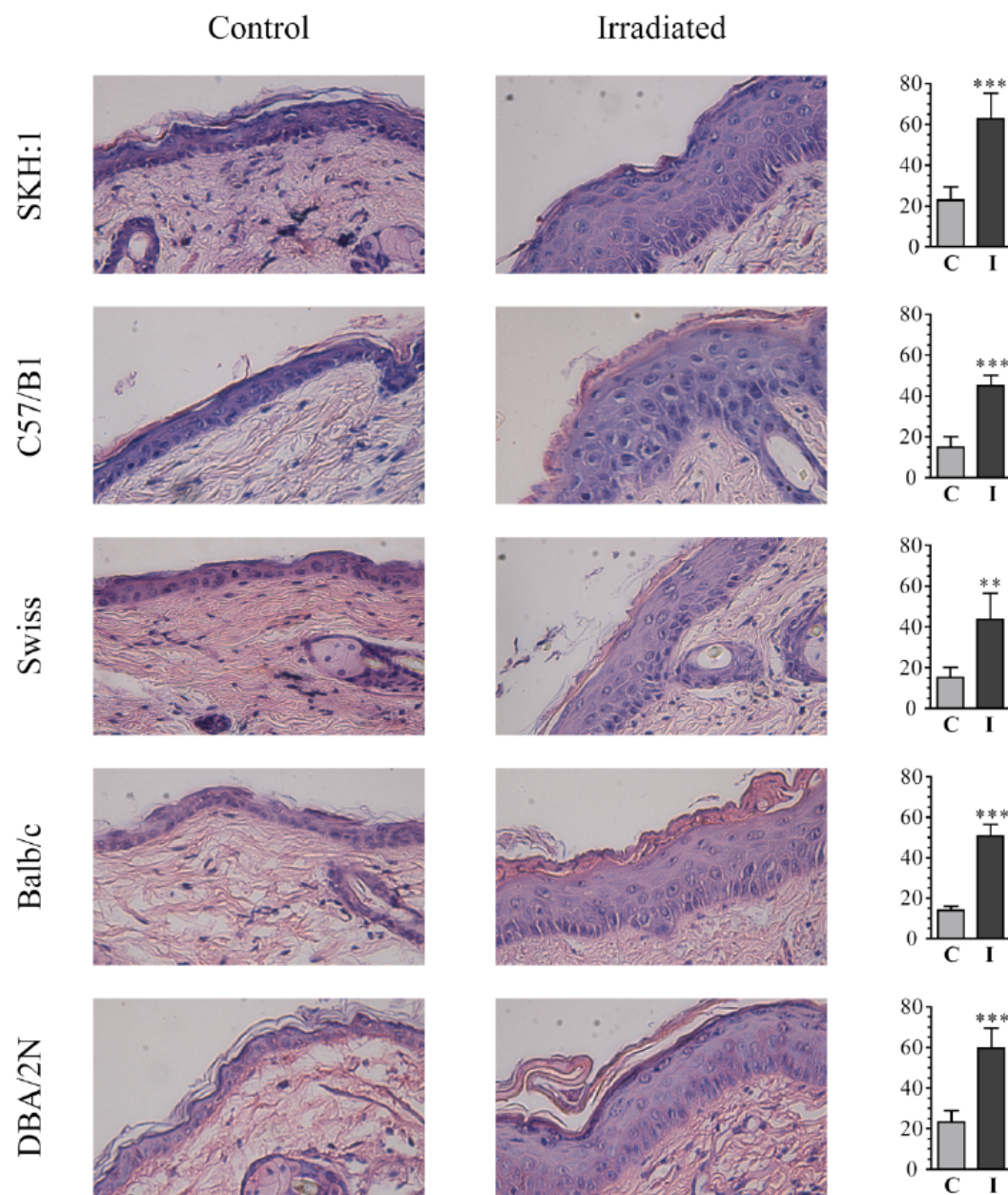


Figure 1: Epidermal histological aspect is shown in a photomicrograph for one control and one irradiated mouse per strain. Quantification of epidermal thickness (μm) is shown in bar graphs. Statistical analysis was performed using a Student t-test, ** $p<0.01$, *** $p<0.001$.

strain. Histogram marker used for quantification of DiOC_6^+ cells is also shown. The percentage of cells bearing polarized mitochondria after irradiation was significantly decreased in all mice strains. However, while some irradiated mice strains like SKH:1, C57/BL and DBA/2N reached very low percentages of this kind of cells (12.0, 7.5 and 6.0, respectively), in UV-exposed Balb/c mice the values decreased just to a 39.5% of these metabolically active cells. DiOC_6^+ cell percentage ranged between 33.8% (DBA/2N) and 78.4% (Balb/c) in unirradiated control mice. Balb/c control mice showed the highest levels of metabolically active cells

followed by SKH:1, which also had high levels of these cells. On the other hand, less than a half of total epidermal cells in DBA mice showed metabolically active mitochondria (Table 1).

Mitochondrial O_2^- Production

Figure 3 shows representative histograms of total epidermal cells' red fluorescence (MitoSOX probe) of one control and one irradiated mouse for each mice strain. Mitochondrial O_2^- production by total epidermal cells, quantified using the marker shown in the figure, was significantly increased in SKH:1 and Balb/c

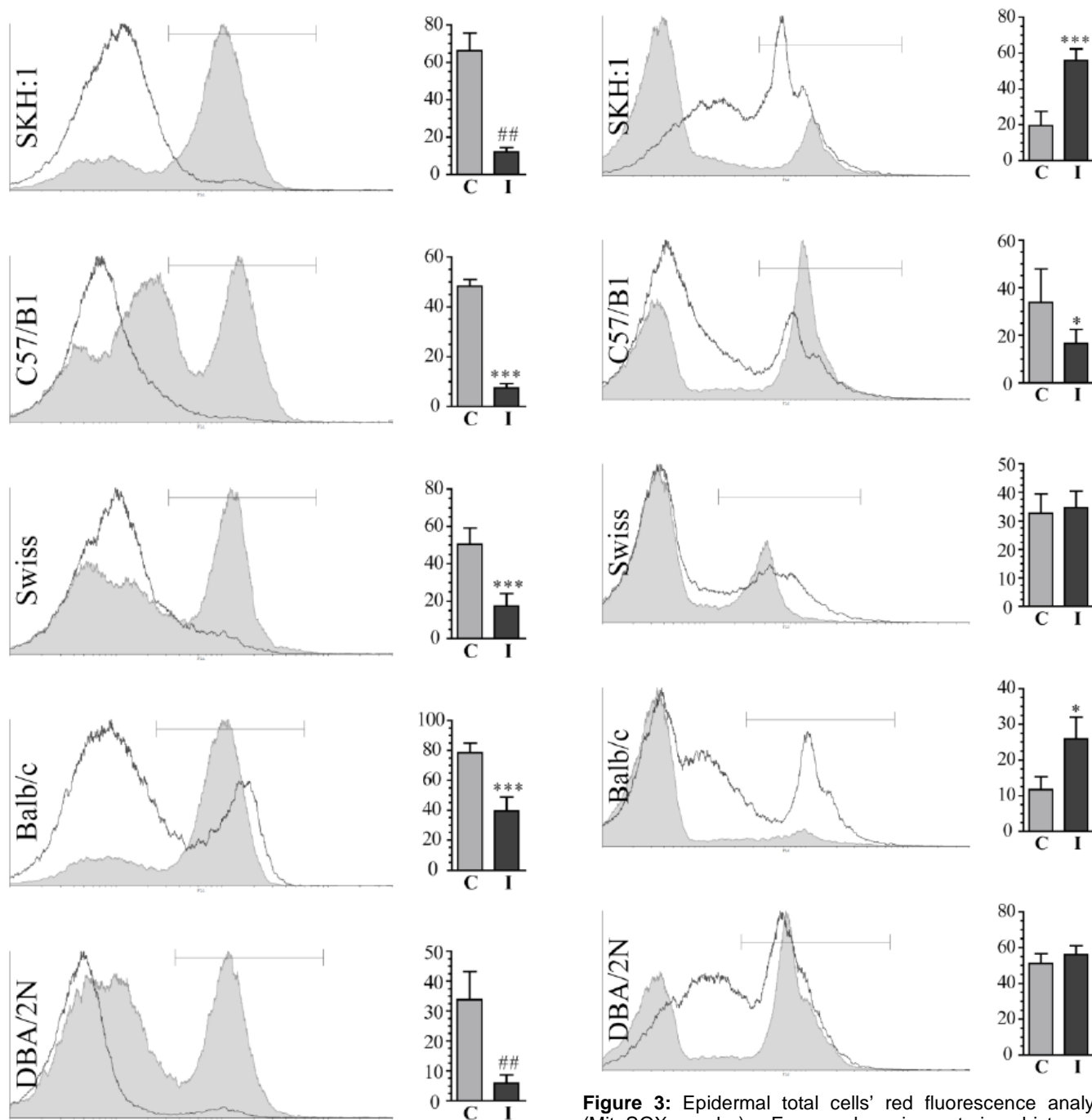


Figure 2: Epidermal total cells' green fluorescence analysis (DiOC₆ probe). For each mice strain, histograms corresponding to one control (solid grey) and one irradiated (black line) mouse are shown. The marker used to quantify DiOC₆⁺ cells is also shown. Quantification of cells bearing polarized mitochondria (% of total epidermal cells) is shown in bar graphs. Statistical analysis was performed using a parametric Student t-test (*) or a nonparametric Mann-Witney test (#), ** or ## p<0.01, *** p<0.001 (n=5).

irradiated mice, while it was unaffected in Swiss and DBA/2N. On the other hand it was significantly decreased in C57/BL, compared to unirradiated control mice.

Figure 3: Epidermal total cells' red fluorescence analysis (MitoSOX probe). For each mice strain, histograms corresponding to one control (solid grey) and one irradiated (black line) mouse are shown. The marker used to quantify MitoSOX⁺ cells is also shown. Quantification of O₂[•] producing cells (% of total epidermal cells) is shown in bar graphs. Statistical analysis was performed using Student t-test, *p<0.05, *** p<0.001 (n=5).

This parameter ranged between 11.7% (Balb/c) and 51.1% (DBA/2N) in unirradiated control mice, showing important differences between mice strains in their basal metabolic state.

Mitochondrial O₂[•] production by metabolically active cells (DiOC₆⁺ cells) is shown in Figure 4. Contrary to

total epidermal cells mitochondrial O_2^- production, when a particular subpopulation of epidermal cells is analyzed (those bearing polarized mitochondria), a significant increase in the production of this free radical was observed in all mice strains.

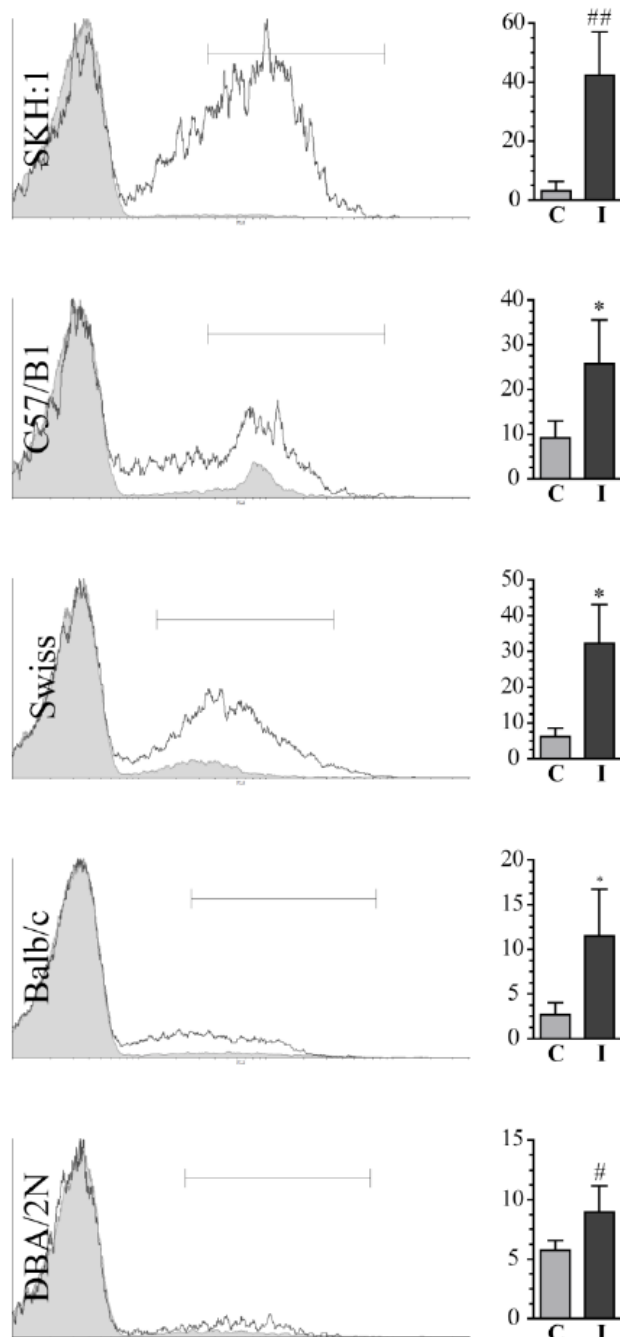


Figure 4: Epidermal DiOC₆⁺ cells' red fluorescence analysis (MitoSOX probe). For each mice strain, histograms corresponding to one control (solid grey) and one irradiated (black line) mouse are shown. The marker used to quantify MitoSOX⁺ cells is also shown. Quantification of O_2^- production by metabolically active cells (% of DiOC₆⁺ cells) is shown in bar graphs. Statistical analysis was performed using a parametric Student t-test (*) or a nonparametric Mann-Witney test (#), * or # p<0.05, ## p<0.01 (n=5).

In control mice, this parameter ranged between 2.7 % (Balb/c) and 9.2 % (C57/BL) (Table 1).

Inflammatory Cytokines Quantification

Figure 5 shows the quantification of the inflammatory cytokines TNF- α and IL-6 in serum (Figures 5a and 5c, respectively) and epidermal homogenates (Figures 5b and 5d, respectively) of irradiated and unirradiated control mice from all strains. A significant increase in serum IL-6 was observed in all irradiated mice strains, with the greatest increments for C57/BL and Swiss mice (138.4 and 94.7 pg/ml, respectively). No changes were observed for serum TNF- α . On the other hand, in epidermal homogenates, a significant increase in TNF- α production was observed in irradiated C57/BL and DBA/2N, compared to their corresponding control group. No changes were observed for epidermal IL-6.

DISCUSSION

Skin exposure to UVr leads to a wide variety of molecular and cellular effects, many of them directly related to skin cancer development. Plenty of these effects have been evaluated using mice models along the last 40 years, since the pioneer studies on UV-induced carcinogenesis performed by Dr. Margaret Kripke [20, 21]. Direct effects of UV irradiation on skin, as well as indirect systemic effects, highly depends both on the dose of UVr and the total number of exposures. In this way, acute exposure produces different effects than multiple or long term chronic ones [22, 23]. Long term chronic effects are vastly represented by skin cancer development, which can be evaluated assessing the multiplicity of tumors or tumor growth rate [23]. Since Dr. Kripke's studies, the establishment of an immunosuppressive state in UV-irradiated mice, which leads to a decrease in anti-tumor immunosurveillance, was clearly evidenced. Afterwards, systemic immunosuppression in UV-irradiated mice was vastly studied by the decrease in cutaneous immune reactions to haptens (contact hypersensitivity reaction, CHS), in short-term and unique UV exposure models.

The mice strain used in the evaluation of UVr effects on skin is also a variable not commonly considered, that may bias the results obtained. As a few examples, hairless SKH:1 mice were frequently used in single irradiation and tumor development studies [24-28], Balb/c mice were useful to investigate systemic immunosuppression and tumor development

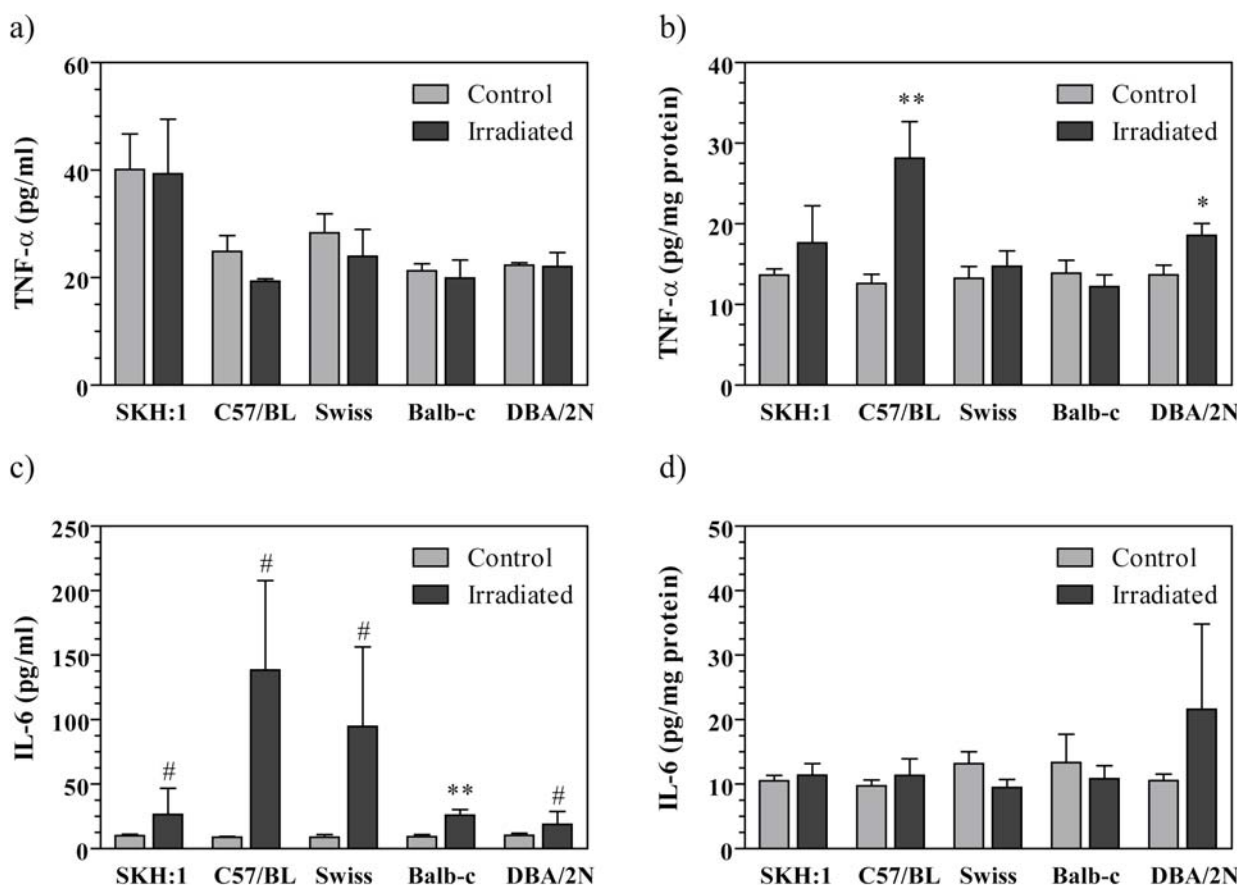


Figure 5: Inflammatory cytokines quantification in serum (a and c) and epidermal homogenates (b and d). Statistical analysis of irradiated groups compared to control was performed for each strain using a parametric Student t-test (*) or a nonparametric Mann-Witney test (#), * or # p<0.05, ** p<0.01 (n=5).

[29-31] as well as C3H mice [32, 33] and, finally, C57BL mice were primarily used for UV-induced immunosuppression mediators studies [34, 35]. However, there are few communications regarding comparative studies between mice strain for particular UVR-induced effects. Sharma *et al.* compared responses of C57BL, SKH:1 and Balb/c to a four-doses scheme of irradiation and found that C57BL mice exhibit a bigger inflammatory response than the other two strains after UV exposure [16]. Moreover, Noonan and Hoffman demonstrated a high susceptibility of the same mice strain for UV-induced immunosuppression, being Balb/c mice more resistant to this effect [17]. In the present work we show both comparable responses between the strains for some effects, and particular ones for others. All mice strains generate an epidermal hyperplasia 72 hours after UVR exposure, showing that general stimuli that promote keratinocyte proliferation are present for all strains. Since keratinocyte hyperproliferation is an important event in skin cancer development, all of the analyzed mice strains may potentially be equally susceptible to it. However, oxidative damage in epidermal cells is quite different

between mice strains. While mitochondrial O₂⁻ production by epidermal cells is increased in irradiated SKH:1 and Balb/c mice, it is not affected in Swiss and DBA mice and is decreased in C57BL mice. According to the relevant role of reactive oxygen species as carcinogenesis promoters [36], we can infer that there may be important differences in tumor susceptibility between mice strains, regarding the amount of oxidative species produced. Moreover, differences in mitochondrial O₂⁻ production between non-irradiated control mice are evident. These differences correlate with the mitochondrial polarization, the less the percentage of cells with polarized mitochondrial, the more the percentage of O₂⁻ producing cells. These differences imply a different susceptibility to oxidative damage between mice strains. Finally, inflammatory responses after UVR exposure also show differences. While C57BL and Swiss irradiated mice show a significant increase in inflammatory mediators (C57BL in epidermis and serum and Swiss only in serum), the other mice strains just produce a slight increase in inflammatory molecules. As the inflammatory profile is related to skin cancer development [37], these different

responses between mice strains are another evidence to consider possible differences in tumor susceptibility between strains.

According to the above presented results, and the ones from other groups, it can be concluded that the selection of a specific mice strain for photodermatology and photoimmunology studies is not a negligible issue and should be carefully done. As results obtained from experiences in these fields are commonly extrapolated to skin cancer development and generalized into relevant species conclusions, the use of one or another mice strain that can bias the conclusions and the usefulness of a particular research should strongly be considered. We finally recommend the comparison of a particular effect in a minimum of two mice strains, before reaching trascendental resolutions.

ACKNOWLEDGEMENTS

This work was supported by a grant of Universidad de Buenos Aires (UBACyT 2011-2013). We would like to thank Ms. Carolina Mourelle and Ms. Angelica Miranda for their technical support and advice in relation to mice care and management.

REFERENCES

- [1] Gibbs NK, Norval M. Urocanic acid in the skin: a mixed blessing? *J Invest Dermatol* 2011; 131: 14-7.
<http://dx.doi.org/10.1038/jid.2010.276>
- [2] Lee J. Molecular events associated with apoptosis and proliferation induced by ultraviolet-B radiation in the skin of hairless mice. *J Dermatol Sci* 2003; 32: 171-9.
[http://dx.doi.org/10.1016/S0923-1811\(03\)00094-X](http://dx.doi.org/10.1016/S0923-1811(03)00094-X)
- [3] Tada-Oikawa S, Oikawa S, Kawanishi S. Role of ultraviolet A-induced oxidative DNA damage in apoptosis via loss of mitochondrial membrane potential and caspase-3 activation. *Biochem Biophys Res Commun* 1998; 247: 693-6.
<http://dx.doi.org/10.1006/bbrc.1998.8869>
- [4] Henseleit U, Rosenbach T, Kolde G. Induction of apoptosis in human HaCaT keratinocytes. *Arch Dermatol Res* 1996; 288: 676-83.
<http://dx.doi.org/10.1007/BF02505277>
- [5] Gonzalez Maglio DH, Paz ML, Ferrari A, et al. Skin damage and mitochondrial dysfunction after acute ultraviolet B irradiation: relationship with nitric oxide production. *Photodermatol Photoimmunol Photomed* 2005; 21: 311-7.
<http://dx.doi.org/10.1111/j.1600-0781.2005.00185.x>
- [6] Paz ML, González Maglio DH, Weill FS, Bustamante J, Leoni J. Mitochondrial dysfunction and cellular stress progression after ultraviolet B irradiation in human keratinocytes. *Photodermatol Photoimmunol Photomed* 2008; 24: 115-22.
<http://dx.doi.org/10.1111/j.1600-0781.2008.00348.x>
- [7] Assefa Z, Vantieghem A, Garmyn M, et al. p38 mitogen-activated protein kinase regulates a novel, caspase-independent pathway for the mitochondrial cytochrome c release in ultraviolet B radiation-induced apoptosis. *J Biol Chem* 2000; 275: 21416-21.
<http://dx.doi.org/10.1074/jbc.M002634200>
- [8] Nicolò C, Tomassini B, Rippo MR, Testi R. UVB-induced apoptosis of human dendritic cells: contribution by caspase-dependent and caspase-independent pathways. *Blood* 2001; 97: 1803-8.
<http://dx.doi.org/10.1182/blood.V97.6.1803>
- [9] Chen AC, Halliday GM, Damian DL. Non-melanoma skin cancer: carcinogenesis and chemoprevention. *Pathology* 2013; 45: 331-41.
<http://dx.doi.org/10.1097/PAT.0b013e32835f515c>
- [10] Kim KH, Park EJ, Seo YJ, et al. Immunohistochemical study of cyclooxygenase-2 and p53 expression in skin tumors. *J Dermatol* 2006; 33: 319-25.
<http://dx.doi.org/10.1111/j.1346-8138.2006.00076.x>
- [11] Gonzalez Maglio DH, Cela EM, Ferrari A, Leoni J. Mitochondrial function evaluation in epidermal cells *ex vivo* after ultraviolet irradiation. *Exp Dermatol* 2011; 20: 947-50.
<http://dx.doi.org/10.1111/j.1600-0625.2011.01342.x>
- [12] Paz ML, Ferrari A, Weill FS, Leoni J, Gonzalez Maglio DH. Time-course evaluation and treatment of skin inflammatory immune response after ultraviolet B irradiation. *Cytokine* 2008; 44: 70-7.
<http://dx.doi.org/10.1016/j.cyto.2008.06.012>
- [13] Köck A, Schwarz T, Kirnbauer R, et al. Human keratinocytes are a source for tumor necrosis factor alpha: evidence for synthesis and release upon stimulation with endotoxin or ultraviolet light. *J Exp Med* 1990; 172: 1609-14.
<http://dx.doi.org/10.1084/jem.172.6.1609>
- [14] Harrison GI, Young AR. Ultraviolet radiation-induced erythema in human skin. *Methods* 2002; 28: 14-9.
[http://dx.doi.org/10.1016/S1046-2023\(02\)00205-0](http://dx.doi.org/10.1016/S1046-2023(02)00205-0)
- [15] Pennello G, Devesa S, Gail M. Association of Surface Ultraviolet B Radiation Levels with Melanoma and Nonmelanoma Skin Cancer in United States Blacks. *Cancer Epidemiol Biomarkers Prev* 2000; 9: 291-7.
- [16] Sharma MR, Werth B, Werth VP. Animal models of acute photodamage: comparisons of anatomic, cellular and molecular responses in C57BL/6J, SKH1 and Balb/c mice. *Photochem Photobiol* 2011; 87: 690-8.
<http://dx.doi.org/10.1111/j.1751-1097.2011.00911.x>
- [17] Noonan FP, Hoffman HA. Susceptibility to immunosuppression by ultraviolet B radiation in the mouse. *Immunogenetics* 1994; 39: 29-39.
<http://dx.doi.org/10.1007/BF00171794>
- [18] Golde WT, Gollobin P, Rodriguez LL. A rapid, simple, and humane method for submandibular bleeding of mice using a lancet. *Lab Anim (NY)* 2005; 34: 39-43.
<http://dx.doi.org/10.1038/laban1005-39>
- [19] COUNCIL DIRECTIVE of 24 November 1986 on the approximation of laws, regulations and administrative provisions of the Member States regarding the protection of animals used for experimental and other scientific purposes (86/609/EEC) [Internet]. 1986; Available from: http://ec.europa.eu/food/fs/aw/aw_legislation/scientific/86-609-eec_en.pdf
- [20] Kripke ML. Antigenicity of murine skin tumors induced by ultraviolet light. *J Natl Cancer Inst* 1974; 53: 1333-6.
- [21] Fisher MS, Kripke ML. Systemic alteration induced in mice by ultraviolet light irradiation and its relationship to ultraviolet carcinogenesis. *Proc Natl Acad Sci* 1977; 74: 1688-92.
<http://dx.doi.org/10.1073/pnas.74.4.1688>
- [22] Weill FS, Cela EM, Ferrari A, Paz ML, Leoni J, Gonzalez Maglio DH. Skin Exposure to Chronic But Not Acute UV Radiation Affects Peripheral T-Cell Function. *J Toxicol Environ Health A* 2011; 74: 838-47.
- [23] Weill FS, Cela EM, Paz ML, Ferrari A, Leoni J, González Maglio DH. Lipoteichoic acid from Lactobacillus rhamnosus GG as an oral photoprotective agent against UV-induced carcinogenesis. *Br J Nutr* 2013; 109: 457-66.
<http://dx.doi.org/10.1017/S0007114512001225>

- [24] Wilgus TA, Ross MS, Parrett ML, Oberyszyn TM. Topical application of a selective cyclooxygenase inhibitor suppresses UVB mediated cutaneous inflammation. *Prostaglandins Other Lipid Mediat* 2000; 62: 367-84.
[http://dx.doi.org/10.1016/S0090-6980\(00\)00089-7](http://dx.doi.org/10.1016/S0090-6980(00)00089-7)
- [25] Hatton JL, Parent A, Tober KL, et al. Depletion of CD4+ cells exacerbates the cutaneous response to acute and chronic uvb exposure. *J Invest Dermatol* 2007; 127: 1507-15.
<http://dx.doi.org/10.1038/sj.jid.5700746>
- [26] Fischer SM, Lo HH, Gordon GB, et al. Chemopreventive activity of celecoxib, a specific cyclooxygenase-2 inhibitor, and indomethacin against ultraviolet light-induced skin carcinogenesis. *Mol Carcinog* 1999; 25: 231-40.
[http://dx.doi.org/10.1002/\(SICI\)1098-2744\(199908\)25:4<231::AID-MC1>3.0.CO;2-E](http://dx.doi.org/10.1002/(SICI)1098-2744(199908)25:4<231::AID-MC1>3.0.CO;2-E)
- [27] Pentland P, Schoggins JW, Scott GA, Khan KN, Han R. Reduction of UV-induced skin tumors in hairless mice by selective COX-2 inhibition. *Carcinogenesis* 1999; 20: 1939-44.
<http://dx.doi.org/10.1093/carcin/20.10.1939>
- [28] Tober KL, Wilgus TA, Kusewitt DF, Thomas-ahner JM, Maruyama T, Oberyszyn TM. Importance of the EP1 Receptor in Cutaneous UVB-Induced Inflammation and Tumor Development. *J Invest Dermatol* 2006; 126: 205-11.
<http://dx.doi.org/10.1038/sj.jid.5700014>
- [29] Budiyanto A, Ahmed NU, Wu A, et al. Protective effect of topically applied olive oil against photocarcinogenesis following UVB exposure of mice. *Carcinogenesis* 2000; 21: 2085-90.
<http://dx.doi.org/10.1093/carcin/21.11.2085>
- [30] Garssen J, de Gruijl F, Mol D, de Klerk A, Roholl P, Van Loveren H. UVA Exposure Affects UVB and cis-Urocanic Acid-Induced Systemic Suppression of Immune Responses in Listeria monocytogenes-infected. *Photochem Photobiol* 2001; 73: 432-8.
[http://dx.doi.org/10.1562/0031-8655\(2001\)073<0432:UEAUAC>2.0.CO;2](http://dx.doi.org/10.1562/0031-8655(2001)073<0432:UEAUAC>2.0.CO;2)
- [31] Gorman S, Tan JW-Y, Thomas JA, et al. Primary defect in UVB-induced systemic immunomodulation does not relate to immature or functionally impaired APCs in regional lymph nodes. *J Immunol* 2005; 174: 6677-85.
- [32] Schwarz A, Maeda A, Wild MK, et al. Ultraviolet radiation-induced regulatory T cells not only inhibit the induction but can suppress the effector phase of contact hypersensitivity. *J Immunol* 2004; 172: 1036-43.
- [33] Ullrich SE, Kripke ML. Mechanisms in the suppression of tumor rejection produced in mice by repeated UV irradiation. *J Immunol* 1984; 133: 2786-90.
- [34] Zhang Q, Yao Y, Konger RL, et al. UVB radiation-mediated inhibition of contact hypersensitivity reactions is dependent on the platelet-activating factor system. *J Invest Dermatol* 2008; 128: 1780-7.
<http://dx.doi.org/10.1038/sj.jid.5701251>
- [35] Wang L, Jameson SC, Hogquist K a. Epidermal Langerhans cells are not required for UV-induced immunosuppression. *J Immunol* 2009; 183: 5548-53.
<http://dx.doi.org/10.4049/jimmunol.0900235>
- [36] Waris G, Ahsan H. Reactive oxygen species: role in the development of cancer and various chronic conditions. *J Carcinog* 2006; 5: 14.
<http://dx.doi.org/10.1186/1477-3163-5-14>
- [37] Aggarwal BB, Shishodia S, Sandur SK, Pandey MK, Sethi G. Inflammation and cancer: how hot is the link? *Biochem Pharmacol* 2006; 72: 1605-21.
<http://dx.doi.org/10.1016/j.bcp.2006.06.029>

Received on 06-11-2013

Accepted on 22-11-2013

Published on 05-03-2014

DOI: <http://dx.doi.org/10.12970/2310-998X.2014.02.01.2>

© 2014 Friedrich et al.; Licensee Synergy Publishers.

This is an open access article licensed under the terms of the Creative Commons Attribution Non-Commercial License (<http://creativecommons.org/licenses/by-nc/3.0/>) which permits unrestricted, non-commercial use, distribution and reproduction in any medium, provided the work is properly cited.